Chiang Mai J. Sci. 2016; 43(2) : 329-338
http://epg.science.cmu.ac.th/ejournal/
Contributed Paper

Kinetics Studies of Non-Isothermal Melt Crystallization of Poly(ε-caprolactone) and Poly(L-lactide)

Wanich Limwanich [a], Sawarot Phetsuk [b], Puttinan Meepowpan [b], Nawee Kungwan [b], Winita Punyodom*[b]

[a] Faculty of Sciences and Agricultural Technology, Rajamangala University of Technology Lanna, Chiang Mai 50300, Thailand.

[b] Polymer Research Laboratory, Department of Chemistry, Faculty of Science, Chiang Mai University, Chiang Mai 50200, Thailand.

*Author for correspondence; e-mail: winitacmu@gmail.com

Received: 15 September 2015
Accepted: 1 November 2015

ABSTRACT

The non-isothermal melt crystallization kinetics of the synthesized poly(ε-caprolactone) (PCL) and poly(L-lactide) (PLL) with identical number average molecular weight ($\overline{M}_n = 1.8\times10^4$) and polydispersity index (PDI = 1.8) was studied by differential scanning calorimetry (DSC). The crystallizations of PCL and PLL were performed under the cooling rates of 5.0, 7.5, 10.0 and 12.5 °C.min^{-1}. From non-isothermal DSC analysis, the crystallization rates increased with increasing of the cooling rates, while the crystallization time decreased for both polymers. The Avrami, Ozawa and Liu models were applied to describe non-isothermal crystallization and determine kinetic parameters for PCL and PLL crystallizations. From Avrami, Ozawa and Liu models, the crystallization mechanism of PCL and PLL was nucleation with three dimensional growths. From Avrami, Liu and Friedman analysis, the synthesized PCL crystallized faster than PLL with the identical molecular weight and PDI value.

Keywords: crystallization, kinetics, differential scanning calorimetry (DSC), poly(L-lactide), poly(ε-caprolactone), biodegradable polymer

1. INTRODUCTION

Poly(ε-caprolactone) (PCL) and poly (L-lactide) (PLL), the biodegradable and biocompatible polymers, are widely used in biomedical applications and packaging materials [1-2]. They have been approved by food and drug administration (FDA) as a safe substance that can be used in the human body since their products from degradation were nontoxic [3-4]. PCL and PLL are generally prepared by ring-opening polymerization (ROP) of ε-caprolactone (ε-CL) and L-lactide (LL), respectively using metal alkoxide initiators [4-5]. It is important to understand the crystallization behavior of these polymers because it affects various properties of polymers such as the

bioresorption, degradation rate, physical and mechanical properties [6-9]. For example, Glauser and co-workers [7] studied the effect of crystallinity on the deformation mechanism and bulk mechanical properties of PLL. They found that amorphous PLL deformed through crazing in the dry, wet and degraded states. Tsuji and Ikada [9] reported the properties of pure PLL membrane at several temperatures. They found that the property of PLL membrane depended strongly on the crystallinity. Moreover, the stress and modulus increased with increasing crystallinity but tension decreased. Therefore, understanding of the crystallization kinetics is necessary for identifying crystallization behavior of polymeric materials since the obtained kinetic parameters can provide the factors that affect properties of polymer such as crystalline melting temperature (T_m), heat of melting (ΔH_m), and %crystallinity, which are important for processing conditions [9-10]. The crystallization kinetics of PCL and PLL has been reported in the literatures [8-15].

However, to the best of our knowledge, there are no reports about the comparison of the crystallization behavior of PCL and PLL with the identical molecular weight and polydispersity index. In order to understand the kinetics of the crystallization of PCL and PLL, the differential scanning calorimetry (DSC) is employed to determine the liberated heat from crystallization process [12-13]. By analyzing the data collected from DSC, the kinetic parameters of crystallization process such as the crystallization rate ($dX(T)/dt$), rate constant of crystallization ($K(T)$) and activation energy (E_a) can be obtained. We also describe the mechanism of non-isothermal crystallizations of PCL and PLL using Avrami, Ozawa and Liu models. The results obtained from all models will be compared and discussed. Finally, the dependency of E_a with relative crystallinity ($X(T)$) is investigated by Friedman isoconversional method.

2. MATERIALS AND METHODS

2.1 Materials Preparation

PCL (number average molecular weight ($\overline{M}_n$) = 1.8×10^4 and polydispersity index (PDI) = 1.83) and PLL (= 1.8×10^4 and PDI = 1.89) were synthesized from ROP of purified ε-CL (Acros Organics, 99.0%) and LL (synthesized from L-lactic acid (Grand Chemical Far East, 88.0%)) using the method described in our previous work [16]. The chemical structures of PCL and PLL are illustrated in Figure 1.

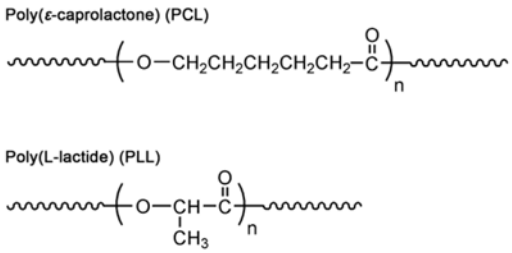

Figure 1. The chemical structures of PCL and PLL.

2.2 DSC Measurements

For crystallization kinetic studies employing Perkin Elmer DSC-7 differential scanning calorimeter, approximately 3 mg of PCL and PLL were weighed into aluminum pan and then hermetically sealed. For PCL crystallization, the samples were firstly heated from 20.0 °C to 80.0 °C at heating rate of 10.0 °C.min^{-1}and held at 80.0 °C for 3 minutes to remove all thermal histories. After that, the molten PCL was cooled from 80.0 °C to 20.0 °C at the cooling rates of 5.0, 7.5, 10.0 and 12.5 °C.min^{-1}. In the case of PLL, the samples were heated from 20.0 °C to 200.0 °C at heating rate of 10.0 °C.min^{-1}and held at 200.0 °C for 3 minutes similar to PCL. Then, the PLL at melt state was cooled from 200.0 °C to

20.0 °C at the cooling rates of 5.0, 7.5, 10.0 and 12.5 °C.min^{-1}. Finally, the crystallized PCL and PLL were heated from 20.0 °C to 80.0 and 200.0 °C, respectively, at heating rate of 10.0 °C.min^{-1} to determine the crystalline melting temperature (T_m) and heat of melting (ΔH_m).

3. RESULTS AND DISCUSSION

3.1 Non-isothermal Crystallizations of PCL and PLL

In this work, we used PCL and PLL with the same molecular weight and PDI values to reduce the variation on the kinetic parameters calculation because the molecular weight of polymer dictates the crystallization rate as reported in literatures [6]. The non-isothermal DSC curves for the crystallization of the molten PCL and PLL at different cooling rates are displayed in Figure 2. It can be seen that the crystallization exotherms shift to lower temperature range and become wider as cooling rate increases. These generally occur for the crystallization of pure polymers or polymer blends [8, 10, 11-13].

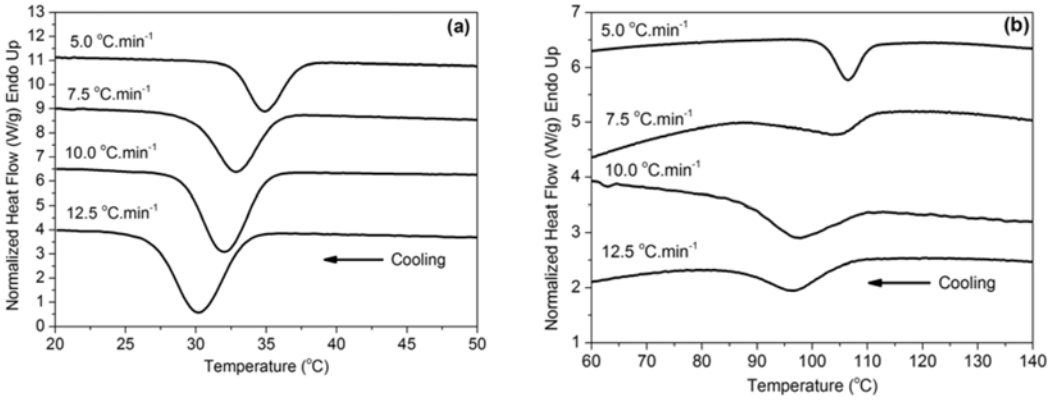

Figure 2. Non-isothermal DSC curves for PCL (a) and PLL (b) crystallizations at the cooling rates of 5, 7.5, 10 and 12.5 °C.min^{-1}.

From the released heat during crystallization, the relative crystallinity ($X(T)$) can be determined from Equation (1) [8].

$$X(T) = \frac{\int_{To}^{T} \left(\frac{dH_c}{dT}\right) dT}{\int_{To}^{T\infty} \left(\frac{dH_c}{dT}\right) dT} \quad (1)$$

where $X(T)$ is the temperature dependence relative crystallinity and dH_c is the measurable heat released from crystallization for infinitesimal range of temperature (dT). Plots of $X(T)$ against temperature and time for PCL and PLL crystallizations are illustrated in Figure 3. Under non-isothermal condition, the crystallization time must be normalized by cooling rate before comparing the crystallization of polymers [17].

From Figure 3 (a, c), it is found that at the highest cooling rate, the $X(T)$ reaches 1 at the lowest temperature compared to those of lower cooling rates [8]. When $X(T)$ is plotted against time shown in Figure 3 (b, d), at the higher cooling rate, the $X(T)$ approached 1 faster than those of lower cooling rates due to the fast crystallization of PCL and PLL. The plots of both systems show sigmoid shape indicating the fast crystallization of primary stage and the slower of secondary stage which are the fact of the nucleation and growth of polymer crystal [18].

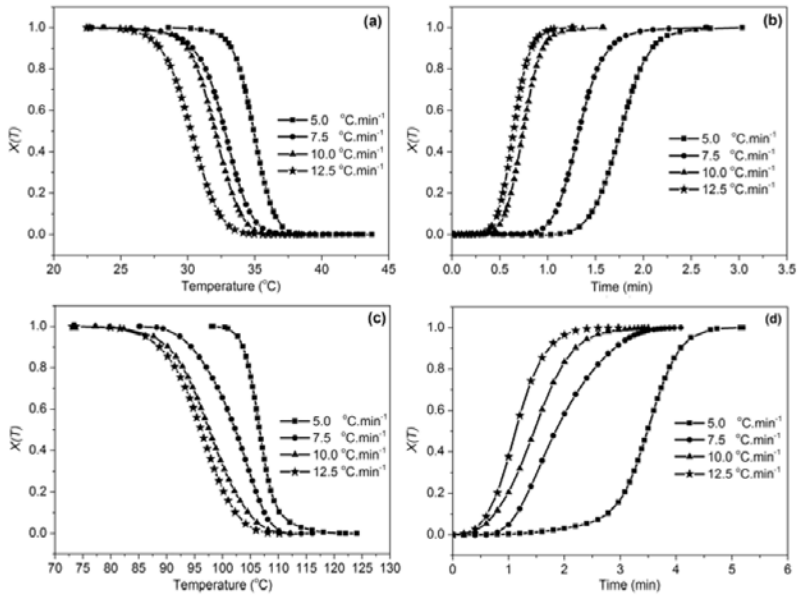

Figure 3. Plots of $X(T)$ against crystallization temperature and time for PCL (a, b) and PLL (c, d) crystallizations at the cooling rates of 5, 7.5, 10 and 12.5 °C.min^{-1}.

To investigate the influence of cooling rate on the values of T_m and ΔH_m of the crystallized PCL and PLL, the DSC melting curves for PCL and PLL displayed in Figure 4(a) and 4(b) are utilized. After the second heating, the PCL melting curves show only one peak but PLL exhibit two peaks which may be corresponded to the different crystal sizes of PLL suggesting the self-nucleation of short PLL chains. Moreover, the second heating DSC curves do not show the cold crystallization exotherms indicate that the PCL and PLL are fully crystallized from melt state under the condition used in this work. The results show the values of T_m of PCL and PLL around 50-60 °C and 140-170 °C, respectively. Furthermore, the values of ΔH_m obtained from both polymers (PCL = 64.5-74.7 J/g and PLL = 43.0-59.2 J/g) seem to decrease with increasing of cooling rate. The mechanism of non-isothermal crystallization of PCL and PLL can be described using Avrami, Ozawa and Liu models. The results obtained from all models will be compared and discussed as follow.

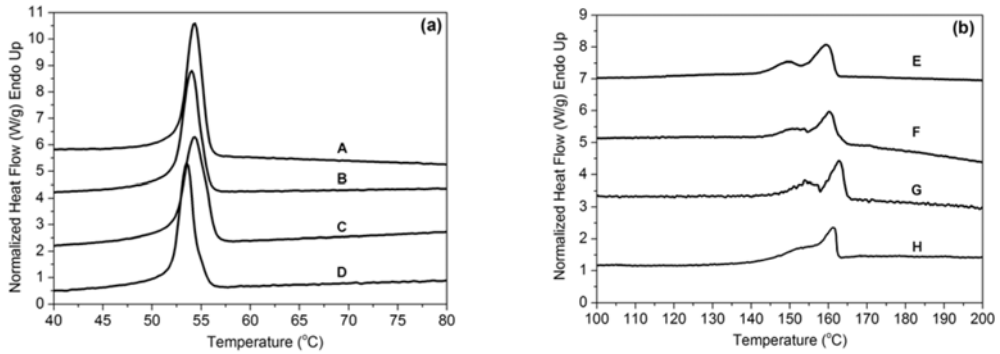

Figure 4. The DSC melting curves for PCL (a) and PLL (b) cooled down with the cooling rates of 5.0 (A, E), 7.5 (B, F), 10.0 (C, G) and 12.5 (D, H) °C.min^{-1}.

Avrami Model

Concerning about crystallization mechanism, Avrami model as shown in Equation (2) is used to determine the Avrami exponent (n), which can describe the crystallization mechanism as reported in literatures [8, 19].

$$\ln(-\ln(1-X(T))) = n\ln t + \ln K(T) \quad (2)$$

where n is the Avrami exponent and $K(T)$ is the crystallization rate constant in the non-isothermal crystallization process. For non-isothermal condition, the logarithmic of $K(T)$ is divided by cooling rate (λ) shown in Equation (3), where K_c is the modified crystallization rate constant [20]. From the Equation (3), the half life of crystallization ($t_{1/2} = (\ln 2/K_c)^{1/n}$) can be calculated.

$$\log K_c = \frac{\log K(T)}{\lambda} \quad (3)$$

The plots of $\ln(-\ln(1-X(T))$ against $\ln t$ are shown in Figure 5. In order to determine the Avrami exponent (n), the $X(T)$ values ($\%X(T) < 60\%$) from the primary crystallization stage of PCL and PLL for all heating rates are utilized [21].

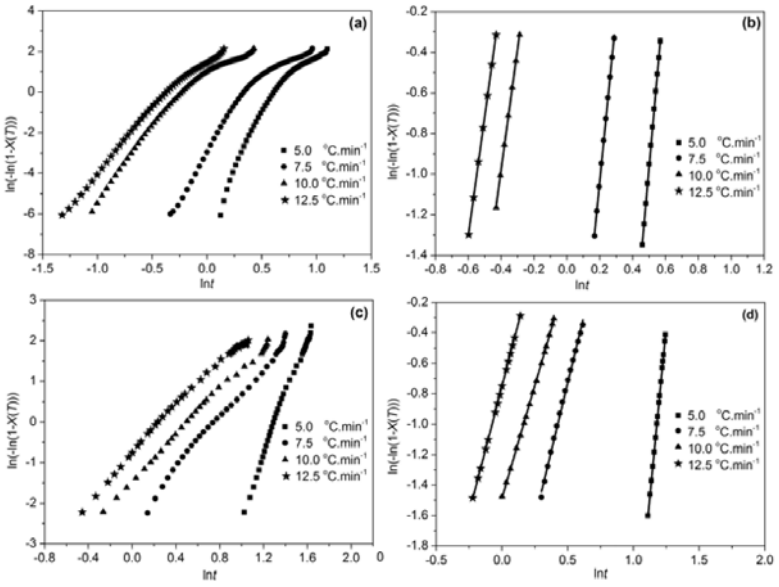

Figure 5. Plots of $\ln(-\ln(1-X(T))$ against $\ln t$ for the whole crystallizations of PCL and PLL (a, c) and plots of $\ln(-\ln(1-X(T))$ against $\ln t$ for the early stage of crystallizations of PCL and PLL (b, d).

The obtained kinetic parameters: the heat of crystallization (ΔH_c), the onset temperature of crystallization (T_0), the Avrami exponent (n), the crystallization rate constant ($K(T)$) and the half life of crystallization ($t_{1/2}$) are summarized in Table 1. The values of n decrease as the cooling rate increases whereas $K(T)$ is found to increase as the cooling rate increases, that causes the decreasing of the time required for 50% of crystallization is reached. By considering $K(T)$, it is found that the values of $K(T)$ of PCL crystallization are higher than PLL suggesting the higher crystallization rate of PCL.

Table 1. The obtained Avrami kinetic parameters from non-isothermal crystallizations of PCL and PLL at the cooling rates of 5.0, 7.5, 10.0 and 12.5 °C.min^{-1}.

Samples	λ (°C.min^{-1})	ΔH_c (J.g^{-1})	T_0 (°C)	n	$K(T)$ ($\times 10^{-3}$)	$t_{1/2}$ (min)
PCL	5.0	74.1	43.7	9.1	3.9	1.01
	7.5	74.9	42.7	8.3	68.0	0.98
	10.0	75.6	39.5	5.9	405.0	0.93
	12.5	66.6	38.3	5.9	9280.0	0.93
PLL	5.0	48.4	124.1	8.4	1.9	1.24
	7.5	32.2	116.1	3.6	81.0	0.99
	10.0	49.5	112.1	3.0	223.0	0.93
	12.5	28.7	110.2	3.3	472.0	0.91

For PCL crystallization, the high values of n (> 4) are obtained implying that the crystallization mechanism starts with a nucleation process and follows by complex three dimensional growths similar to literatures [8, 21]. The values of n > 4 may be caused by an increasing of the rate of nucleation indicating the different growth mechanisms occur throughout the crystallization process of PCL. Furthermore, the Avrami plots for PCL crystallization at high relative crystallinity (> 80%) deviate from a linear behavior as shown in Figure 5(a). This deviation is caused by a slower crystallization rate occurring in the secondary crystallization stage of PCL. The decreasing of crystallization rate may be caused by the change of the crystallization mechanism. In the case of PLL crystallization shown in Table 1, the determined n value at low cooling rate of 5 °C.min^{-1} was 8.4 indicating the complex three dimensional growths of PLL crystal similar to PCL.

The PCL and PLL crystallizations from the melt state under non-isothermal condition to the crystalline state can be explained by the simple model as illustrated in Figure 6. At melt state ($T > T_m$), the PCL and PLL chains are in the amorphous phase due to the high energy, free volume, chain mobility, chain rotation, *etc.* These cause them not able to orient and rearrange themselves to form the crystal structure. After removing of all thermal history at melt state, PCL and PLL are cooled down ($T < T_m$) to induce the crystallization. At this stage, PCL and PLL chains have lower energy that causes the decreasing of chain mobility and free volume between chains. Then, the nucleation is occurred by some parts of chains are oriented to crystalline phase with high chain order. After the nucleation process, the PCL and PLL crystal growth by the more connected and ordered chains at crystalline region. Finally, the three dimensional growths of PCL and PLL are formed.

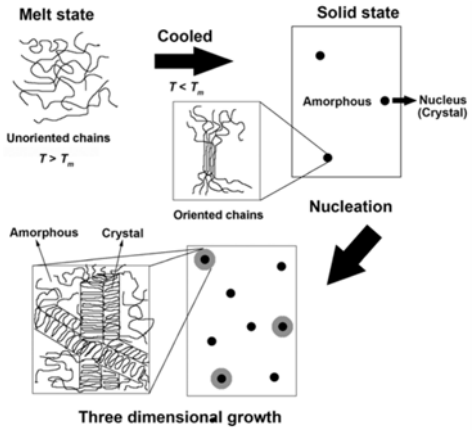

Figure 6. The crystallizations of PCL and PLL with nucleation and growth mechanism under non-isothermal condition.

Ozawa Model

The Ozawa model is the alternative approach to describe the crystallization mechanism of polymeric materials based on Avrami theory. Ozawa modified Avrami equation to explain the non-isothermal crystallization for a molten polymer sample cooled at a constant cooling rate as shown in Equation (4) [22].

$$1 - X(T) = \exp\left[\frac{-K(T)}{\lambda^m}\right] \quad (4)$$

where m is the Ozawa exponent which depends on the dimensions of the crystal growth. $K(T)$ is the crystallization rate constant. The validity of Ozawa method can be determined from the linearity of double logarithmic plots of ln(-ln(1-$X(T)$)) against lnλ as shown in Figure 7. The results show that this model fails to describe the crystallization of PCL due to the nonlinear plots as shown in Figure 7(a) [11]. However, the Ozawa plots for PLL crystallization at 100-109 °C showed a good linear correlation ($R^2 > 0.97$) suggesting that this model is satisfied to describe the non-isothermal crystallization of PLL. The average m value for PLL crystallization about 4 indicates the crystallization mechanism is complex three dimensional growths similar to Avrami analysis.

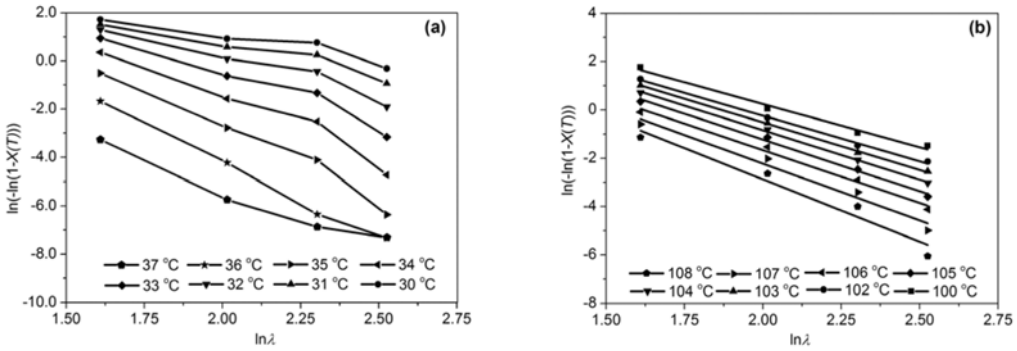

Figure 7. Plots of ln(-ln(1-$X(T)$)) against lnλ based on Ozawa model for non-isothermal crystallizations of PCL (a) and PLL (b).

Liu Model

The better model for describing the non-isothermal crystallization of polymeric materials is Liu model [23]. Liu and co-workers combine the Avrami and Ozawa equations with the assumption that the degree of crystallinity is corrected to λ and temperature (or time). The combined Avrami and Ozawa equations are shown in the following equation.

$$\ln\lambda = \ln F(T) - \alpha \ln t \quad (5)$$

where the parameter $F(T) = (k(T)/K)^{1/m}$ is the necessary value of λ to reach a defined degree of crystallinity at unit crystallization time and α is the ratio of Avrami (n) and Ozawa exponents (m), where $\alpha = n/m$. According to Equation (5), at a constant X_t, the plots of lnλ against ln$t$ for PCL and PLL crystallizations (Figure 8) show a good linear behavior with $R^2 > 0.95$ and 0.97, respectively. This indicates that Liu model can well describe the non-isothermal crystallization of PCL and PLL. The values of α and $F(T)$ are determined from the slope and intercept of these plots, respectively and summarized in Table 2.

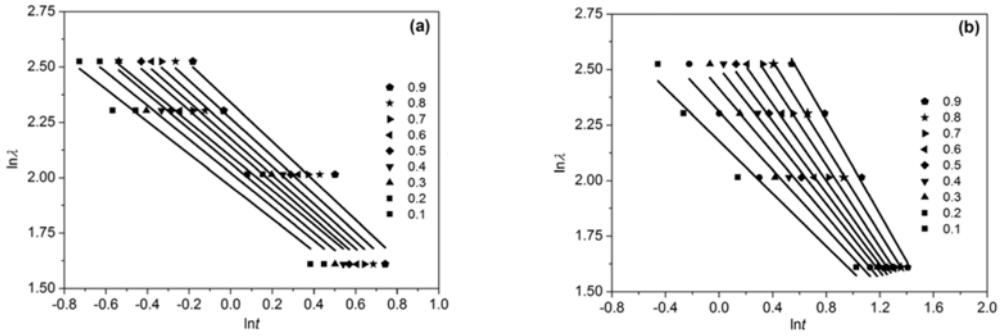

Figure 8. Plots of lnλ against ln$t$ based on Liu model for non-isothermal crystallizations of PCL (a) and PLL (b).

The results show the increasing of α and $F(T)$ with X_t similar to literature [11]. The increasing of $F(T)$ for both polymers indicating the higher cooling rates are needed to achieve high crystallinity at the same time. Moreover, the higher $F(T)$ values of PLL than PCL suggest that the crystallization rate of PLL is lower than PCL [24]. Furthermore, the data obtained from Liu model will be supported by the values of activation energy (E_a) determined from Friedman isoconversional method.

Table 2. The non-isothermal crystallization kinetics parameters of PCL and PLL obtained from Liu model.

X_t	PCL			PLL		
	α	$F(T)$	R^2	α	$F(T)$	R^2
0.1	0.732	7.105	0.950	0.592	8.832	0.968
0.2	0.762	7.548	0.953	0.659	10.087	0.966
0.3	0.783	7.883	0.952	0.716	11.177	0.967
0.4	0.772	8.143	0.957	0.766	12.275	0.974
0.5	0.816	8.511	0.952	0.809	13.351	0.982
0.6	0.827	8.814	0.952	0.861	14.699	0.989
0.7	0.841	9.187	0.953	0.924	16.585	0.996
0.8	0.857	9.659	0.950	0.972	18.681	0.999
0.9	0.882	10.375	0.950	1.061	22.667	0.996

Activation Energy Determination by Friedman Isoconversional Method

From the obtained non-isothermal kinetics data, the dependency of E_a with $X(T)$ is determined using the well known Friedman isoconversional method [11, 25]. This method employs the relationship of the natural logarithm of reaction rate, ln(dα/dt), as a function of the reciprocal temperature to provide the E_a for each fraction of conversion (α) as shown in Equation (6).

$$\ln\left(\frac{d\alpha}{dt}\right) = \ln(Af(\alpha)) - \frac{E_\alpha}{RT} \quad (6)$$

where A is the frequency factor and $f(\alpha)$ is the function of conversion. Therefore, E_a can be simply obtained from the slope of the plot of -ln(dα/dt) against 1000/T. The dependency of E_a with $X(T)$ are illustrated in Figure 9. The results show the

higher values of E_a (less negative) for PLL crystallization indicating the lower crystallization rate than PCL. This lower crystallization rate of PLL is caused by the steric effect of methyl (CH_3) side group of PLL chain that reduces the chain connection. The results from Friedman isoconversional analysis are similar to the results obtained from Avrami and Liu models

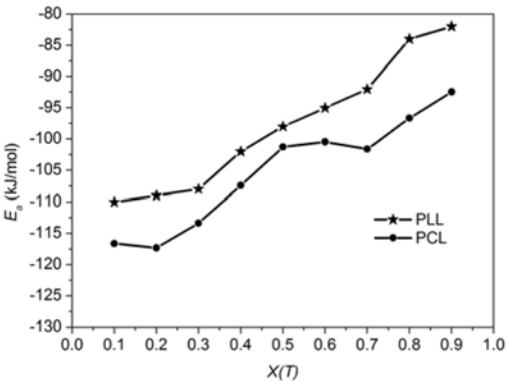

Figure 9. Plots of E_a against $X(T)$ for PCL and PLL crystallizations obtained from Friedman isoconversional methods.

4. CONCLUSIONS

The PCL and PLL with identical molecular weight (M_n= 1.8×10^4) were successfully synthesized using the ROP of ε-CL and LL, respectively. The crystallization kinetics of PCL and PLL was investigated by non-isothermal DSC technique and the crystallization mechanism was analyzed by Avrami, Ozawa and Liu models. These three models are suitable to describe the crystallization kinetic of PLL, however the Ozawa model fails to describe the crystallization kinetic of PCL. The obtained results from three models suggest that the mechanisms of PCL and PLL crystallizations under non-isothermal condition are nucleation process with complex three dimensional growths. Moreover, the E_a values obtained by Friedman isoconversional method for PCL crystallization are lower than those of PLL crystallization. Furthermore, the average E_a values for PCL and PLL crystallization are -100 and -85 kJ/mol, respectively. The results from this work may be useful for other systems such as copolymers or polymer blends of PCL and PLL.

ACKNOWLEDGEMENTS

This research work was supported by CMU-Mid-Career Research Fellowship Program (for WP and SP). SP would like to thank the Research Professional Development Project under the Science Achievement Scholarship of Thailand (SAST) for graduate fellowship. Department of Chemistry, Faculty of Science and Graduate School of Chiang Mai University and Rajamangala University of Technology Lanna (RMUTL), Chiang Mai were also acknowledged.

REFERENCES

[1] Albertsson A.C., Varma I.K., *Biomacromolecules*. 2003; **4**: 1466-1486.

[2] Wu J., Yu T.L., Chen C.T., Lin C.C., *Coord. Chem. Rev.*, 2006; **250**: 602-606.

[3] Vassiliou A.A., Papageorgiou G.Z., Achilias D.S., Bikiaris D.N., *Macromol. Chem. Phys.*, 2007; **208**: 364-376.

[4] Stridsberg K.M., Ryner M., Albertsson A.C., *Adv. Polym. Sci.*, 2002; **157**: 41-65.

[5] Coulembier O., Degee P., Herrick J.L., Dubois P., *Prog. Polym. Sci.*, 2006; **31**: 723-747.

[6] He Y., Fan Z., Hu Y., Wu T., Wei J., Li S., *Eur. Polym. J.*, 2007; **43**: 4431-4439.

[7] Annette C., Renouf G., John R., David F.F., Ruth E.C., *Biomaterials*, 2005; **26**: 5771-5782.

[8] Wang X.L., Huang F.Y., Zhou Y., Wang Y.Z., *J. Macromol. Sci. B.,* 2009; **48**: 710-722.

[9] Tsuji H., Ikada Y., *Polymer*, 1995; **6**: 2709-2716.

[10] Salmeron S.M., Gomez R.J.L., Hernandez S.F., Mano J.F., *Thermochim. Acta*., 2005; **430**: 201-210.

[11] Dhanvijay P.U., Shertukede V.V., Kalkar A.K., *J. Appl. Polym. Sci.*, 2012; **124**: 1333-1343.

[12] Liu Y., Wang L., He Y., Fan Z., Li S., *Polym. Int.*, 2010; **59**: 1616-1621.

[13] Ravari F., Mashak A., Nekoomanesh M., Mobedi H., *Polym. Bull.*, 2013; **70**: 2569-2586.

[14] Miyata T., Masuko T., *Polymer*, 1998; **39**: 5515-5521.

[15] Jenkins M.J., Harrison K.L., *Polym. Adv. Technol.*, 2006; **17**: 474-478.

[16] Limwanich W., Khunmanee S., Kungwan N., Punyodom W., *Thermochim. Acta,* 2015; **599**: 1-7.

[17] Li J., Zhou C. X., Wang G., Tao Y., Liu Q., Li Y., *Polym. Test.*, 2002; **21**: 583-589.

[18] Mya K.Y., Pramoda K.P., He C.B., *Polymer*, 2006; **47**: 5035-5043.

[19] Avrami M., *J. Chem. Phys.*, 1939; **7**: 1103-1112.

[20] Jeziorny A., *Polymer*, 1978; **19**: 1142-1144.

[21] Kuo M.C., Huang J.C., Chen M., *Mater. Chem. Phys.*, 2006; **99**: 258-268.

[22] Ozawa T., *Polymer*, 1971; **12**: 150-158.

[23] Liu T., Mo Z., Wang S., Zhang H., *Polym. Eng. Sci.*, 1997; **37**: 568-575.

[24] Zeng J.B., Srinivansan M., Li S.L., Narayan R., Wang Y.Z., *Ind. Eng. Chem. Res.*, 2011; **50**: 4471-4477.

[25] Friedman H.L., *J. Polym. Sci. Part C: Polym. Sym.*, 1964; **6**: 183-195.